University of Wollongong

Research Online

2020

Triboelectric Nanogenerator versus Piezoelectric Generator at Low Frequency (<4 >Hz): A Quantitative Comparison

Abdelsalam Ahmed

Islam Hassan

Ahmed Helal

Vitor Sencadas
University of Wollongong, victors@uow.edu.au

Ali Radhi

See next page for additional authors

Triboelectric Nanogenerator versus Piezoelectric Generator at Low Frequency (<4 >Hz): A Quantitative Comparison

Abstract

© 2020 The Author(s) Triboelectric nanogenerators (TENGs) and piezoelectric generators (PGs) are generally considered the two most common approaches for harvesting ambient mechanical energy that is ubiquitous in our everyday life. The main difference between the two generators lies in their respective working frequency range. Despite the remarkable progress, there has been no quantitative studies on the operating frequency band of the two generators at frequency values below 4 Hz, typical of human motion. Here, the two generators are systematically compared based on their energy harvesting capabilities below 4 Hz. Unlike PGs, the TENG demonstrates higher power performance and is almost independent of the operating frequency, making it highly efficient for multi-frequency operation. In addition, PGs were shown to be inapplicable for charging capacitors when a rectifier was attached to the system. The results of this work reveal the tremendous potential of flexible TENGs for harvesting energy at low frequency.

Keywords

generator, piezoelectric, versus, comparison, nanogenerator, quantitative, triboelectric, hz):, (<4, frequency, low

Disciplines

Engineering | Science and Technology Studies

Publication Details

Authors

Abdelsalam Ahmed, Islam Hassan, Ahmed Helal, Vitor Sencadas, Ali Radhi, Chang Jeong, and Maher El-Kady

Article

Triboelectric Nanogenerator versus Piezoelectric Generator at Low Frequency (<4 Hz): A Quantitative Comparison
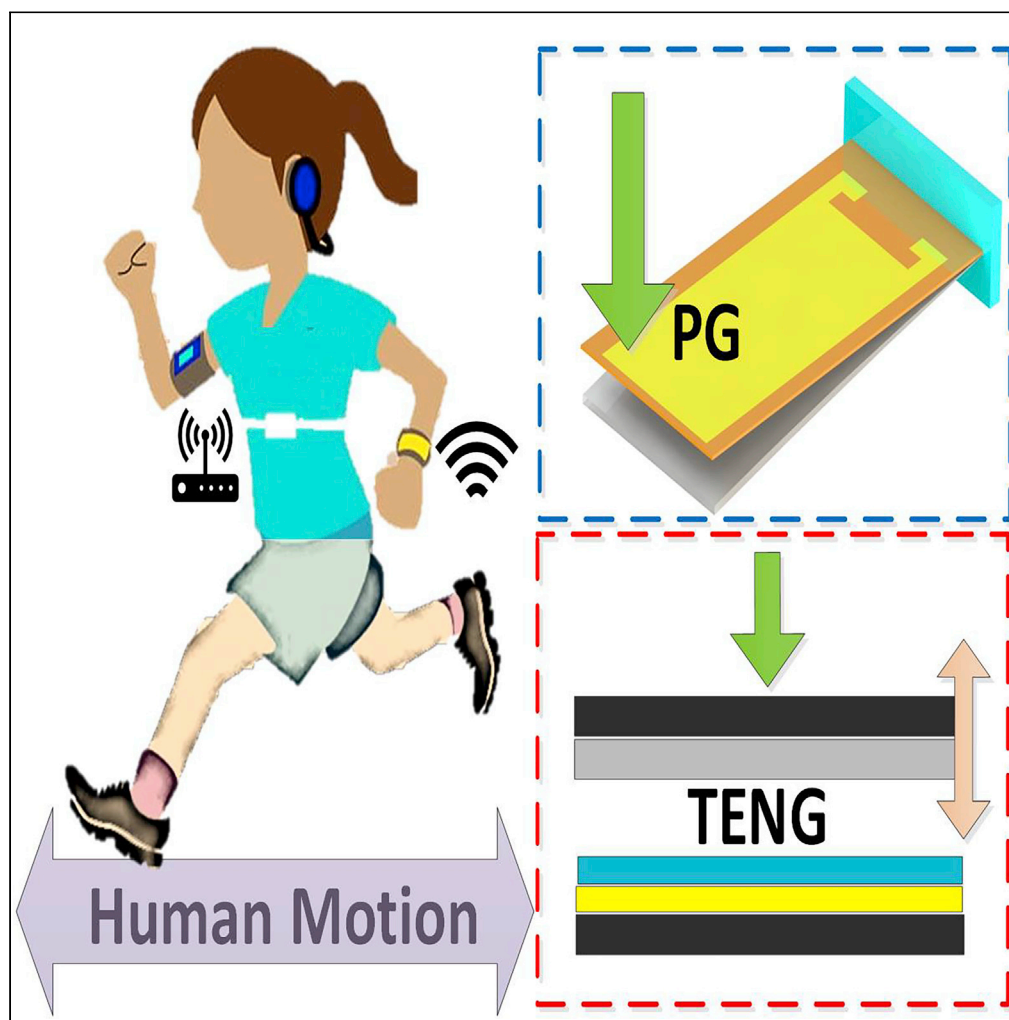
Abdelsalam Ahmed, Islam Hassan, Ahmed S. Helal, Vitor Sencadas, Ali Radhi, Chang Kyu Jeong, Maher F. El-Kady

aahmed26@bwh.harvard.edu

HIGHLIGHTS

This work presents a systematic comparative study between PGs and TENGs below 4 Hz

Unlike PGs, the TENG demonstrates higher power performance at low-frequency range

Also, PGs was shown to be inapplicable for charging capacitors when a rectifier was used

This work reveals the tremendous potential of TENGs as an energy harvester

Article

Triboelectric Nanogenerator versus Piezoelectric Generator at Low Frequency (<4 Hz): A Quantitative Comparison

Abdelsalam Ahmed,[1,2,12,13,*] Islam Hassan,[3,7,12] Ahmed S. Helal,[4] Vitor Sencadas,[1,5,6] Ali Radhi,[7] Chang Kyu Jeong,[8,9] and Maher F. El-Kady[10,11]

SUMMARY

Triboelectric nanogenerators (TENGs) and piezoelectric generators (PGs) are generally considered the two most common approaches for harvesting ambient mechanical energy that is ubiquitous in our everyday life. The main difference between the two generators lies in their respective working frequency range. Despite the remarkable progress, there has been no quantitative studies on the operating frequency band of the two generators at frequency values below 4 Hz, typical of human motion. Here, the two generators are systematically compared based on their energy harvesting capabilities below 4 Hz. Unlike PGs, the TENG demonstrates higher power performance and is almost independent of the operating frequency, making it highly efficient for multi-frequency operation. In addition, PGs were shown to be inapplicable for charging capacitors when a rectifier was attached to the system. The results of this work reveal the tremendous potential of flexible TENGs for harvesting energy at low frequency.

INTRODUCTION

Small-scale electronics has boomed during the last decade for the Internet of Things (IoT), wireless sensor networks (WSNs), smart city design, and medical application (Gubbi et al., 2013; Jaladi et al., 2017). The components of such devices typically require a minimal amount of power, but it becomes a challenge when considering a large network of devices reaching up to billions. Moreover, maintenance cost may explode as the number of distributed micro-electronics increases when considering existing battery-based electronics, where their batteries are prone to replacements after its service life. The field of energy harvesting tries to answer these challenges by developing energy conversion schemes from ambient energy existing in the ecosystem such that electrical output is generated to allow for self-powered electronics (Mateu et al., 2005; Elvin and Erturk, 2013). In particular, mechanical energy is known for its abundance in the surrounding environment, readily available for potential energy harvesting apparatus based on electromagnetic (Yang et al., 2009), piezoelectric (Kim et al., 2011; Wang, 2008), triboelectric (Wang, 2013; Ahmed et al., 2019b) (Ahmed et al., 2020a), or electrostatic (Boisseau et al., 2012). Of these approaches, triboelectric nanogenerators (TENGs) and piezoelectric generators (PGs) have more significant potential for applications and were hybridized and coupled on numerous occasions during the past few years (Ahmed et al., 2017b, Ahmed et al., 2017; Chen et al., 2017).

The available mechanical energy found in the environment typically experiences low-frequency behaviors (around 10 Hz and lower). Examples of such mechanical motion are abundantly found in oceanic waves, human motion, wind currents, and other wildlife species (Naruse et al., 2009; Salauddin and Park, 2017). Harvesting such low-frequency sources may not be the best when utilizing piezoelectric technologies because PGs are known to be efficient at higher frequency ranges (60–100 Hz and above) (Liu et al., 2018; Han et al., 2013). The recent research effort has been dedicated to broadening the operating frequency range of PGs to include low-frequency loads (Wang, 2017; Jeong et al., 2017a). However, there are significant obstacles that still pose a challenge for PGs to reach such extremely low levels of mechanical frequencies (<10 Hz or sub 1 Hz frequencies). On the other hand, TENGs, owing to their attractive attributes, have been successfully applied for harvesting all kinds of mechanical energy such as vibration, human body motion, animal organs wind power, and water motion (Yang et al., 2013; Ahmed et al., 2017a, 2017c, 2017d, Ahmed et al., 2017, 2017f, Ahmed et al., 2018, 2019a, 2019c, 2019d, 2020b). A theoretical comparison between TENGs

[1]Department of Mechanical Engineering, Massachusetts Institute of Technology, Cambridge, MA, USA

[2]Division of Gastroenterology, Brigham and Women's Hospital, Harvard Medical School, Boston, MA, USA

[3]Department of Mechanical Engineering, McMaster University, Hamilton, ON, Canada

[4]Department of Nuclear Science and Engineering, Massachusetts Institute of Technology, Cambridge, MA, USA

[5]School of Mechanical, Materials, Mechatronic and Biomedical Engineering, University of Wollongong, Wollongong, NSW 2500, Australia

[6]ARC Centre of Excellence for Electromaterials Science, University of Wollongong, Wollongong, NSW 2500, Australia

[7]Department of Mechanical and Industrial Engineering, University of Toronto, Toronto, ON, Canada

[8]Division of Advanced Materials Engineering, Jeonbuk National University, Jeonju, Jeonbuk 54896, Republic of Korea

[9]Hydrogen and Fuel Cell Research Center, Jeonbuk National University, Jeonju, Jeonbuk 54896, Republic of Korea

[10]Department of Chemistry and Biochemistry and California NanoSystems Institute, University of California, Los Angeles (UCLA), Loss Angeles, CA, USA

[11]Department of Materials Science and Engineering, UCLA, Los Angeles, CA, USA
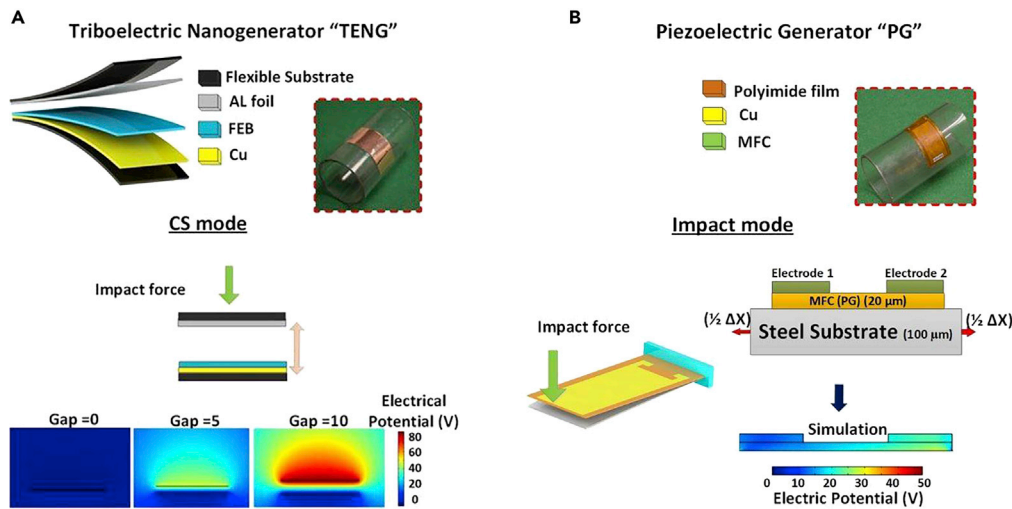
Continued

Figure 1. Direct Comparison of the Operation Modes and FEM Modeling of TENG and PG, Respectively
Schematic illustration, photograph of the fabricated devices, and EFM modeling for (A) TENG and (B) PG devices.

and PGs was previously conducted and reported by Han et al., 2015. However, a quantitative comparison has not been conducted yet regarding the operating frequency band between the two generators from low-frequency mechanical excitations.

Here, we present a comparative study and analysis between TENGs and PGs on low-frequency mechanical energy harvesting. In order to achieve a more systematic comparison, a simplified design of the TENG is compared with a chosen commercial PG. Contact separation (CS) TENG was fabricated, whereas the PG was made to operate in similar operating mode (Impact mode "IM"). For both energy harvesters, each mode is investigated and their respective open-circuit voltage V_{OC} and short-circuit current I_{SC} are used for electrical output comparison at multiple frequency values <4 Hz. PGs are efficient at much higher frequency values, where their extremely small outputs limit their uses for powering small-electronics or charging capacitors. TENG will be shown to have a maintainable and sustainable voltage and energy values, regardless of the frequency of mechanical excitation. This study shows the high efficiency of TENGS over PGs at a frequency less than 4 Hz for harvesting low-frequency mechanical loads.

RESULTS

This study aims to compare two of the most promising energy harvesting technologies, namely, TENGs and PGs, where they share several attractive features such as relatively low costs, ease of fabrication, and integrability in flexible electronics. CS operating mode is widely used in mechanical energy harvesting owing to their simplicity, efficiency, and compatibility with multi-directional loads (Yang et al., 2013). This mode was carefully selected as our criteria of comparison because it can be applied to both TENGs and PGs at the same time. Moreover, the CS mode was previously coupled in various device configurations owing to their outstanding performance in low-frequency/amplitude excitations. Analogous to TENGs, PGs were set up to have similar operating modes. The set up with CS mode was made possible by exerting an impact load on the PG (IM mode) in a contact-separation manner (Fuh et al., 2015; Gu, 2011). Therefore, this study utilizes the proposed modes as a foundation of systematic comparison between the two generators.

Figure 1A shows active materials and electrodes used for fabricating the TENG. The CS mode harvests energy by contact separation between the fluorinated ethylene propylene (FEB) layer and aluminum (Al) layer. The size and weight of PGs and TENGs are listed in Methods. For the computational part, we conducted both TENG and PG simulations at the same load conditions. Using the Multiphysics COMSOL software, a simulation was conducted to obtain the electrical potential field of the TENG at separation distances of 0, 5, and 10 mm as shown in Figure 1A. When there is no separation between the FEP and Al layers, the ensuing potential field is approximately zero at the interface. At a separation distance of 10 mm, the CS mode generates an electrical potential up to 80 V. Hence, the electrical potential shows a significant

[12]These authors contributed equally

[13]Lead Contact

*Correspondence:
aahmed26@bwh.harvard.edu

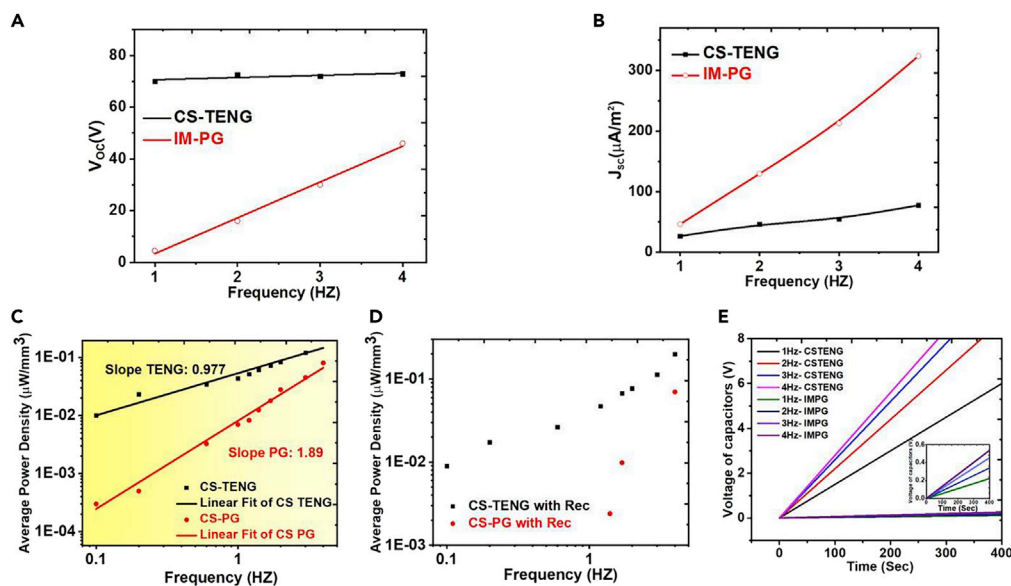https://doi.org/10.1016/j.isci.2020.101286

Figure 2. Evaluation of the Electric Properties and Performance of TENG and PG at Low Frequencies
(A and B) Open circuit voltage and short circuit current for TENG and PG at different frequencies.
(C and D) (C) The average power densities generated at multiple low-frequency values for the two generators. The electrical output performance of the two generators is also shown after connecting to a rectifier for (D) TENG and PG, respectively. Charging performance of a capacitor at multiple operating frequencies is investigated for the two generators.
(E) Charging performance of a capacitor at multiple operating frequencies is investigated for the two generators.

increase with larger separation distances. A computational model was also applied to the PG devices (Park et al., 2017; Jeong et al., 2017b), as shown in Figure 1B. Owing to its remarkable piezoelectric effect, lead zirconate titanate (PZT) ceramic is used in the prototypes of PG devices. This has now been replaced with a Macro Fiber Composite (MFC) in commercial devices as it offers high performance, flexibility, and low cost. The device consists of uniaxial piezoelectric ceramic fibers surrounded by a polymer matrix such as epoxy, which provides protection for the fibers and allows the materials to readily conform to curved surfaces. This unique design combines the power density of piezoceramic materials with the flexibility of polymers. However, a simplified representation of the PG materials is obtained by using PZT as the PG material for simulation, which according to the manufacturer has properties similar to those of MFC (dos Santos Guimarães et al., 2010). The observed piezoelectric field had a consistent distribution of roughly 26 V between adjacent electrodes under impact mode.

Initially, we measured open-circuit voltages V_{oc} and short-circuit currents I_{SC} for both devices, while each measurement is conducted at different mechanical load frequencies. Figure 2 summarizes the results, with a prescribed mechanical motion outlined in Methods. According to data in Figure 2A, TENG shows a highly stable voltage output and is almost independent of the applied frequency, whereas the voltage of PGs increases linearly with the applied frequency. Nevertheless, the PG could only deliver around half the voltage of the TENG even when tested at maximum frequency (4 Hz). Based on the working mechanism of piezoelectric energy harvesters, the frequency-dependent behavior of PG output can be easily addressed. When the mechanical input frequency increases, the electron flow through the external circuit and instrument shows shorter time to respond to the piezo-potential change, then this causes the higher current signal, because the total amount of electron flow should be same. Since the voltage signal is the product of the current and circuital resistance (impedance), the voltage also becomes higher correspondingly. This linear relationship causes PG generators to work only under constant periodic loads and limits their use in a multi-frequency environment (Gu et al., 2012). According to the previous reports, the voltage level can be saturated at a certain input frequency owing to the device structures, measurement conditions, and so on (Gu et al., 2012; Yang et al., 2017). For our comparison study, the measurements were conducted in off-resonance and tapping modes (<5 Hz), showing the frequency-dependent relationship of PG devices (Gu et al., 2012). Furthermore, it is known that PGs generally deliver higher current values
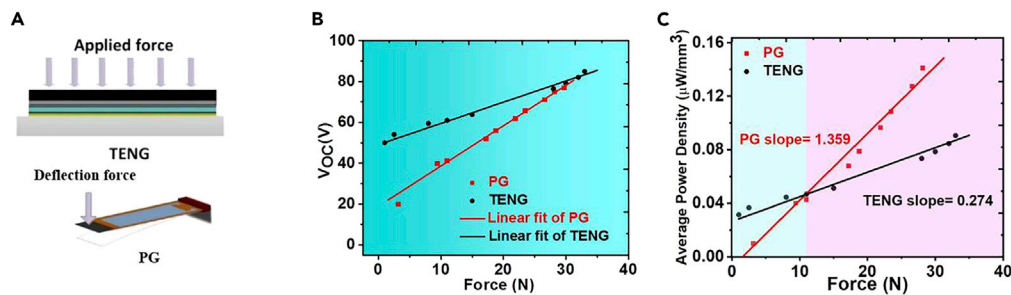
Figure 3. Electrical Performance of TENG and PG as a Function of the Applied Force
(A) Schematic illustration of the TENG and PG under different applied forces.
(B) The measured open-circuit voltages at different applied forces.
(C) The average power densities at different applied forces.

than TENGs, which is also true here as can be seen in Figure 2B. However, the current shows direct proportionality with frequency.

Next, we experimentally demonstrated the average power density (per unit volume) and its correlation with the operating frequency. Figure 2C compares the performance of TENG and PG systems, respectively. Given the wide range of frequencies and power, the data are presented on a logarithmic scale, where the TENG had almost twice the power density of the PG system at the maximum operating frequency for both modes. The slope of the fitted data has been calculated to manifest the consistency of power generation at multiple frequency values. It can be observed that TENGs had a much lower energy density variation than PGs, as lined by the calculated slope. The generated energy of PGs shows a strong dependence on the input frequency, whereas the TENG exhibits stable performance and is less dependent on the applied frequency. As discussed previously, the voltage of PG is proportional to the triggering frequency ω. This corresponds well to the broadband frequency operation of TENGs to sustain operations at multiple frequency levels, as opposed to variable PG outputs.

Figure 2D shows the power density results of each generator after connecting the rectifier. It can be observed that the TENG was able to produce electrical output with frequencies as small as 0.2 Hz. Moreover, this electrical output was still maintained for multiple frequencies after connecting the rectifier. However, PG was only able to produce electrical output at a minimum frequency value of 1 Hz (one order of magnitude higher than the minimum operating frequency of TENG) when connected with a rectifier. This limits the various works of PG harvesters for environments with extremely low frequencies, especially when powering up an electrical component or charging up a battery. Because most of the output power disappears after connecting to a rectifier, the PG harvesters might be impractical for generating or storing sustainable power combined with a rectifying circuit. To ascertain such observations, Figure 2E shows the voltage of charging a capacitor using the two harvesters, respectively, and the time it takes to charge the capacitor at multiple frequency values. Consequently, the previous results show that most of the charge density is omitted for the PG harvesters and the obtained charge is only about half of that reached by TENG-based harvesters at only the maximum frequency. That corresponds well with the current capacitor's voltage results as the PG harvesters are unable to charge the capacitor to a large voltage within the time span of 400 s, reaching a maximum of 0.6 V for PG (see inset in Figure 2E).

Next, we investigate the effect of load magnitude on the energy harvesting performance for the two generator types as portrayed in Figure 3A. Figure 3B shows the open-circuit voltage results, for the two generators with a linear fit of the data. The TENG experienced much higher voltages at lower values of applied loads, where the PG performance approaches that of the TENG as the load magnitude increases. To verify the power performance of the two harvesters, the generated power was calculated for the two cases and compared in Figure 3C. At very low regions, the TENG performed well at a load range of approximately 10 N and below. The 10 N mark represents a break-even point, above which the PG starts to outperform TENGs thanks to the superior power performance of the PG device, which seems to increase more rapidly with the applied force, as shown in Figure 3C.
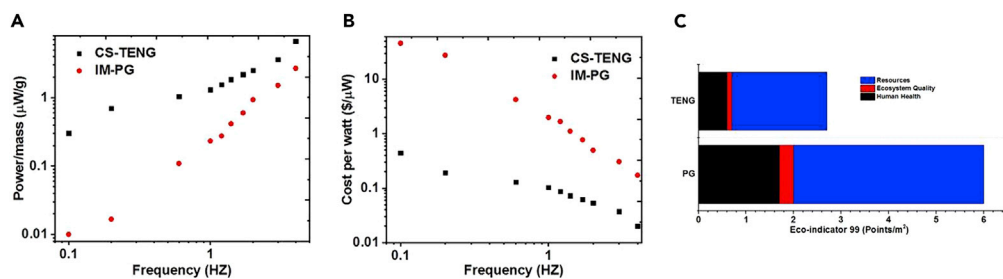
Figure 4. Specific Power, Cost per Watt, and Techno-Economic Analysis of TENG and PG
(A) The average power-to-mass ratio of PG and TENG.
(B) The cost per watt of PG and TENG.
(C) Eco-indicator 99 results for 1 m^2 of each mode. The data for TENG is extracted from the study of Ahmed et al., 2017.
The data for PG is extracted from the study of Ibn-Mohammed et al. (2016).

It is worth noting that the power performance for the two devices under different loads (Figure 3) follows a different trend from that when tested as a function of the operating frequency of the source (Figure 2). The main difference between the two generators regarding the loading profile is that the PGs were exposed to a point load at the end of the cantilever-like structure, whereas TENGs experienced a distributed load to cover its contact area. Therefore, the maximum deflection of a cantilever beam due to a point load is directly proportional to the load magnitude (Takács, 2012). As such, increased deflection of the PG will create an enhanced electrical output due to the piezoelectric effect. As for, TENGs has experienced an increased slope of average power with elevated mechanical loads. Low distributed loads in a contact-separation motion may not ensure full contact area between the two triboelectric layers. However, additional loads would enhance the contact surface (i.e., increase the total contact area), which would enhance the electrical output from the TENGs and their surface charges.

DISCUSSION

We conducted a comparative analysis of the harvesters' weight and economic performances relative to the produced power. Figures 4A and 4B show the specific power (power normalized to the weight of the device) generated by both energy harvesters. Both TENG and PG exhibit adequate energy harvesting capabilities with a slight advantage to TENGs regarding power generation per unit mass. The specific power experiences an increase with increasing frequency. On the other hand, there is a considerable difference in cost per watt between the two harvesters at extremely low-frequency values (around 1 Hz). At this frequency, the cost of PGs is higher than that of TENGs. However, the cost of PG power goes down very rapidly as the frequency increases. In contrast, the cost of TENGs is relatively constant, making it highly efficient regarding multi-frequency operation at low-frequency scales.

As energy harvesting technologies, the two mechanical generator types should be investigated within a cost-metric context to ascertain their performance regarding the cost of materials, fabrication, and their environmental profiles. Here, we discuss the techno-economic of the TENG (Ahmed et al., 2017) and PG (Ibn-Mohammed et al., 2016), where a chosen metric was assigned with its data presented in Figure 4C. The metric chosen was the Eco-indicator 99, which provides an insight into whether the technologies constitute any significant environmental limitations. The three categories for this comparison were ecosystem quality, resources, and human health. In all three categories, PGs showed higher Eco-indicator 99 (environmental impact) values than TENGs, with a more visible difference coming from resources and human health. The comparative study had shown a general preference for TENGs over PGs when operating in the low frequency/force amplitude regions. This excellent performance opens up the door for a wide range of self-powered electronics for wearable and wireless sensing applications. Such wearable devices would require a minimal effort to operate, charge, and/or activate embedded electronics by mere human motion and surrounding environmental conditions.

In summary, this work presents a systematic comparative study between PGs and TENGs as potential energy harvesting devices operating in low-frequency conditions. In general, PGs exhibit low voltage and high current output, with both V_{OC} and I_{SC} having a visible proportionality with the operating frequency. On the other hand, measurements show that TENGs do experience high voltage outputs with minimal

proportionality to the operating frequency and low current output. These attributes enable TENGs to demonstrate much higher power density compared with PGs along the low-frequency range (below 1 Hz). At these frequency levels, the extremely low voltage values obtained by PGs limit their applications in powering up electronic devices and energy storage units with rectifiers. Moreover, the energy performance against the load magnitude confirmed that the TENGs are superior at lower mechanical loads values. However, break-even analysis shows that PGs are better at higher values within the portrayed load magnitude range. Finally, the work reveals a considerable opportunity for TENGs in wearable, self-powered electronics powered by low-frequency/amplitude mechanical motions associated with human movements.

Limitations of Study

We provide a detail comparison of TENG and PG in low frequency, which is helpful for researchers. However, theoretical investigation can be conducted to get in-depth understanding for both generators under different modes. In addition, different device modes such as, cantilever mode can be used to study different effects on the generator's performance.

Resource Availability

Lead Contact

Abdelsalam Ahmed.

Materials Availability

This study did not generate new unique reagents.

Data and Code Availability

We do not have any code and upon request we can provide the original data.

METHODS

All methods can be found in the accompanying Transparent Methods supplemental file.

SUPPLEMENTAL INFORMATION

Supplemental Information can be found online at https://doi.org/10.1016/j.isci.2020.101286.

AUTHOR CONTRIBUTIONS

A.A., I.H., designed, executed, and analyzed most of the experiments and wrote the manuscript. A.H., I.H., A. H, V.S., A.R., C.J. and M.E. edited the manuscript.

DECLARATION OF INTERESTS

All authors confirm there are no competing interests.

REFERENCES

Ahmed, A., Hassan, I., Hedaya, M., El-Yazid, T.A., Zu, J., and Wang, Z.L. (2017a). Farms of triboelectric nanogenerators for harvesting wind energy: a potential approach towards green energy. Nano Energy *36*, 21–29.

Ahmed, A., Hassan, I., Ibn-Mohammed, T., Mostafa, H., Reaney, I.M., Koh, L.S., Zu, J., and Wang, Z.L. (2017b). Environmental life cycle assessment and techno-economic analysis of triboelectric nanogenerators. Energy Environ. Sci. *10*, 653–671.

Ahmed, A., Hassan, I., Jiang, T., Youssef, K., Liu, L., Hedaya, M., Yazid, T.A., Zu, J., and Wang, Z.L. (2017c). Design guidelines of triboelectric nanogenerator for water wave energy harvesters. Nanotechnology *28*, 185403.

Ahmed, A., Hassan, I., Song, P., Gamaleldin, M., Radhi, A., Panwar, N., Tjin, S.C., Desoky, A.Y., Sinton, D., and Yong, K.-T. (2017d). Self-adaptive bioinspired hummingbird-wing stimulated triboelectric nanogenerators. Sci. Rep. 7, 17143.

Ahmed, A., Zhang, S.L., Hassan, I., Saadatnia, Z., Zi, Y., Zu, J., and Wang, Z.L. (2017f). A washable, stretchable, and self-powered human-machine interfacing Triboelectric nanogenerator for wireless communications and soft robotics pressure sensor arrays. Extreme Mech. Lett. 13, 25–35.

Ahmed, A., El-Kady, M.F., Hassan, I., Negm, A., Pourrahimi, A.M., Muni, M., Selvaganapathy, P.R., and Kaner, R.B. (2019a). Fire-retardant, self-extinguishing triboelectric nanogenerators. Nano Energy 59, 336–345.

Ahmed, A., Hassan, I., El-Kady, M.F., Radhi, A., Jeong, C.K., Selvaganapathy, P.R., Zu, J., Ren, S., Wang, Q., and Kaner, R.B. (2019b). Integrated triboelectric nanogenerators in the era of the Internet of Things. Adv. Sci. 6, 1802230.

Ahmed, A., Hassan, I., Mosa, I.M., Elsanadidy, E., Phadke, G.S., El-Kady, M.F., Rusling, J.F., Selvaganapathy, P.R., and Kaner, R.B. (2019c). All printable snow-based triboelectric nanogenerator. Nano Energy 60, 17–25.

Ahmed, A., Hassan, I., Mosa, I.M., Elsanadidy, E., Sharafeldin, M., Rusling, J.F., and Ren, S. (2019d). An ultra-shapeable, smart sensing platform based on a multimodal ferrofluid-infused surface. Adv. Mater. 31, e1807201.

Ahmed, A., Guan, Y.-S., Hassan, I., Ling, C., Li, Z., Mosa, I., Phadke, G., Selvaganapathy, P.R., Chang, S., and Ren, S. (2020a). Multifunctional smart electronic skin fabricated from two-dimensional like polymer film. Nano Energy, 105044.

Ahmed, A., Hassan, I., and Zu, J. (2018). Design guidelines of stretchable pressure sensors based triboelectrification. Adv. Technol. Mater. 20, 1700997.

Ahmed, A., Saadatnia, Z., Hassan, I., Zi, Y., Xi, Y., He, X., Zu, J., and Wang, Z.L. (2017e). Self-powered wireless sensor node enabled by a duck-shaped triboelectric nanogenerator for harvesting water wave energy. Adv. Energy Mater. 7, 1601705.

Ahmed, A., Shehata, M., Hassan, I., Abdelhak, Y.I., Cigdem, E., El-Kady, M., Ismail, Y., and Mostafa, H. (2020b). A theoretical modeling analysis for triboelectrification controlled light emitting diodes. Nano Energy, 104874.

Boisseau, S., Despesse, G., and Seddik, B.A. (2012). Electrostatic conversion for vibration energy harvesting. Small-Scale Energy Harvesting, 1–39.

Chen, S., Tao, X., Zeng, W., Yang, B., and Shang, S. (2017). Quantifying energy harvested from

contact-mode hybrid nanogenerators with cascaded piezoelectric and triboelectric units. Adv. Energy Mater. 7, 1601569.

dos Santos Guimarães, C., de Silva Bussamra, F.L., Pommier-Budinger, V., and Hernandes, J.A. (2010). Structural Shape Control Using Macro Fiber Composite Piezoelectric Sensors and Actuators (Asociacion Argentina de Mecanica Computacional).

Elvin, N., and Erturk, A. (2013). Advances in Energy Harvesting Methods (Springer Science & Business Media).

Fuh, Y.-K., Chen, P.-C., Huang, Z.-M., and Ho, H.-C. (2015). Self-powered sensing elements based on direct-write, highly flexible piezoelectric polymeric nano/microfibers. Nano Energy 11, 671–677.

Gu, L. (2011). Low-frequency piezoelectric energy harvesting prototype suitable for the MEMS implementation. Microelectron. J. 42, 277–282.

Gu, L., Cui, N., Cheng, L., Xu, Q., Bai, S., Yuan, M., Wu, W., Liu, J., Zhao, Y., and Ma, F. (2012). Flexible fiber nanogenerator with 209 V output voltage directly powers a light-emitting diode. Nano Lett. 13, 91–94.

Gubbi, J., Buyya, R., Marusic, S., and Palaniswami, M. (2013). Internet of Things (IoT): a vision, architectural elements, and future directions. Future Gener. Comp. Sy. 29, 1645–1660.

Han, M., Chen, X., Yu, B., and Zhang, H. (2015). Coupling of piezoelectric and triboelectric effects: from theoretical analysis to experimental verification. Adv. Electron. Mater. 1, 1500187.

Han, M., Zhang, X.-S., Meng, B., Liu, W., Tang, W., Sun, X., Wang, W., and Zhang, H. (2013). r-Shaped hybrid nanogenerator with enhanced piezoelectricity. ACS Nano 7, 8554–8560.

Ibn-Mohammed, T., Koh, S., Reaney, I., Acquaye, A., Wang, D., Taylor, S., and Genovese, A. (2016). Integrated hybrid life cycle assessment and supply chain environmental profile evaluations of lead-based (lead zirconate titanate) versus lead-free (potassium sodium niobate) piezoelectric ceramics. Energy Environ. Sci. 9, 3495–3520.

Jaladi, A.R., Khithani, K., Pawar, P., Malvi, K., and Sahoo, G. (2017). Environmental monitoring using wireless sensor networks (WSN) based on IOT. Int. Res. J. Eng. Technol. 4, 1371–1378.

Jeong, C.K., Cho, S.B., Han, J.H., Park, D.Y., Yang, S., Park, K.-I., Ryu, J., Sohn, H., Chung, Y.-C., and Lee, K.J. (2017a). Flexible highly-effective energy harvester via crystallographic and computational control of nanointerfacial morphotropic piezoelectric thin film. Nano Res. 10, 437–455.

Jeong, C.K., Han, J.H., Palneedi, H., Park, H., Hwang, G.-T., Joung, B., Kim, S.-G., Shin, H.J., Kang, I.-S., and Ryu, J. (2017b). Comprehensive biocompatibility of nontoxic and high-output

flexible energy harvester using lead-free piezoceramic thin film. APL Mater. 5, 074102.

Kim, H.S., Kim, J.-H., and Kim, J. (2011). A review of piezoelectric energy harvesting based on vibration. Int. J. Precis. Eng. Man. 12, 1129–1141.

Liu, H., Zhong, J., Lee, C., Lee, S.-W., and Lin, L. (2018). A comprehensive review on piezoelectric energy harvesting technology: materials, mechanisms, and applications. Appl. Phys. Rev. 5, 041306.

Mateu, L., Echeto, M., and De Borja, F. Review of energy harvesting techniques and applications for microelectronics. Proc. SPIE 5837, VLSI Circuits and Systems II, 2005. International Society for Optical Engineering.

Naruse, Y., Matsubara, N., Mabuchi, K., Izumi, M., and Suzuki, S. (2009). Electrostatic micro power generation from low-frequency vibration such as human motion. J. Micromech. Microeng. 19, 094002.

Salauddin, M. and Park, J. A low frequency vibration driven, miniaturized and hybridized electromagnetic and triboelectric energy harvester using dual Halbach array. Solid-State Sensors, Actuators and Microsystems (TRANSDUCERS), 2017 19th International Conference on, 2017. IEEE, 1832–5.

Park, D.Y., Joe, D.J., Kim, D.H., Park, H., Han, J.H., Jeong, C.K., Park, H., Park, J.G., Joung, B., and Lee, K.J. (2017). Self-powered real-time arterial pulse monitoring using ultrathin epidermal piezoelectric sensors. Adv. Mater. 29, 1702308.

Takács, G. (2012). Basics of Vibration Dynamics. Model Predictive Vibration Control (Springer).

Wang, Z.L. (2008). Self-powered nanotech. Scientific American 298, 82–87.

Wang, Z.L. (2013). Triboelectric nanogenerators as new energy technology for self-powered systems and as active mechanical and chemical sensors. ACS Nano 7, 9533–9557.

Wang, Z.L. (2017). On Maxwell's displacement current for energy and sensors: the origin of nanogenerators. Mater. Today 20, 74–82.

Yang, B., Lee, C., Xiang, W., Xie, J., He, J.H., Kotlanka, R.K., Low, S.P., and Feng, H. (2009). Electromagnetic energy harvesting from vibrations of multiple frequencies. J. Micromech. Microeng. 19, 035001.

Yang, Y., Zhang, H., Lin, Z.-H., Zhou, Y.S., Jing, Q., Su, Y., Yang, J., Chen, J., Hu, C., and Wang, Z.L. (2013). Human skin based triboelectric nanogenerators for harvesting biomechanical energy and as self-powered active tactile sensor system. ACS Nano 7, 9213–9222.

Yang, Z., Erturk, A., and Zu, J. (2017). On the efficiency of piezoelectric energy harvesters. Extreme Mech. Lett. 15, 26–37.

Supplemental Information

Triboelectric Nanogenerator

versus Piezoelectric Generator at Low

Frequency (<4 Hz): A Quantitative Comparison

Abdelsalam Ahmed, Islam Hassan, Ahmed S. Helal, Vitor Sencadas, Ali Radhi, Chang Kyu Jeong, and Maher F. El-Kady

Fabrication of the TENG: A 100 µm thick FEP film (dimensions 18 × 40 mm) was coated with a layer of 200 nm thick Cu electrodes using physical vapor deposition (PVD500) before being attached to the substrate. This was brought in contact with the other electrode, a 100 µm thick Al foil with these dimensions 18 x 60 mm. This stack was sandwiched between two pieces of polyvinyl chloride (PVC, dimension 18 × 40 mm and thickness 0.5 mm) to provide the physical support for the device. The overall weight of the stack was measured to be 3.7g.

Fabrication of PG: The PG device was made by winding a commercial Macro Fiber Composite MFC (28 × 14 mm, model M-2814-P1 from Smart-Material, Corp) around a 0.1 mm thick steel sheet (18 × 40 mm) and is approximately 5 g in weight. The chosen MFC consists of rectangular piezoceramic rods sandwiched between two adhesive layers with an $d_{33} = 460$ pC/N (Smart-Material.com, 2020). In this case, the ceramic is lead zirconate titanate (PZT) with the chemical formula $(Pb[Zr_{(x)}Ti_{(1-x)}]O_3)$, whereas epoxy was used as the connecting polymer matrix. To complete the PG device, the MFC layer is attached to a polyimide film with copper back contact electrodes that are typically applied in an interdigitated pattern.

Electromechanical Measurements: A three-dimensional positioner was used to deploy the nanogenerator (TENG or PG) in the vertical orientation. A force sensor was then attached to the end of a linear motor, enabling precise measurements. In this setup, the output current and voltage data were collected by a voltage preamplifier (Keithley 6514 System Electrometer). We implemented LabVIEW software as a platform for real-time data acquisition and control analysis. In the course of these experiments, different levels of external loads were tested during power measurements. This experiment utilized a linear motor to produce periodic loads with several magnitudes and frequencies. Starting from time t = 0), the motion profile can be expressed as shown below:

$$X = \begin{cases} 8X_{max}f^2t^2 & ; 0 \le t \le \frac{1}{4f} \\ 8X_{max}ft - 8X_{max}f^2t^2 - X_{max} & ; \frac{1}{4f} \le t \le \frac{3}{4f} \\ 8X_{max}f^2(\frac{1}{f} - t)^2 & ; \frac{3}{4f} \le t \le \frac{1}{4f} \end{cases}$$

Simulation and modeling:

TENG: The multiphysics study for the TENG was conducted by COMSOL. The potential field results were obtained between the Al and Cu electrodes, where the model was set up with the original device dimensions with deposited Cu on the FEP film. The film has dimensions of 18 × 40 mm. The floating potential terminal was assigned to the Al electrode with the Cu electrode connected to the ground. Positive and negative triboelectric charge densities were allocated at tens of $\mu C/m^2$ to the Al and FEP layer, respectively.

PG: The model was set with a 20 μm piezoelectric layer and conductive electrodes with PZT as the material model for the piezoelectric simulation [8]. The electrodes were separated by a 200 μm gap. A Young's modulus of 54.05 GPa was selected for the finite element model along with a piezoelectric charge constant d_{33} of 440 pC/N. The active area density ρ and the dielectric constant K_T were set as 5.44 g/cm^3 and 1950, respectively. [9] The applied strain was obtained from the bending radius and the thickness of the multilayer substrate, which is expressed as $\varepsilon = \delta/r$ [10]. This formula is derived from the neutral plane distance from the top surface of the MFC film δ, and the PG bending radius r. This applies to flexible MFC devices containing a plastic surface with an epoxy passivation layer. In the PG simulation, figure 1, the results show the potential field between the electrodes only. Also, the open-circuit voltage contour was outputted without any external loads. The TENG simulation shows the field over its overall dimensions. Identical boundary conditions were utilized for both simulations.